VOL. 17, NO. 9, MAY 2022 ISSN 1819-6608
ARPN Journal of Engineering and Applied Sciences

www.arpnjournals.com

STRUCTURE DYNAMIC ANALYSIS ON MOBILITY ROBOT FOOTREST FOR ADULT MALE

W. H. Tan[1,2], A. B. Shahriman[1,2], C. Y. Teoh[3] and C. H. Lee[1,2]
[1]Motorsport Technology Research Unit and UniMAP Racing Circuit (MoTECH), Pauh Putra Campus, Universiti Malaysia Perlis (UniMAP), Arau, Perlis, Malaysia
[2]Faculty of Mechanical Engineering Technology, Universiti Malaysia Perlis (UniMAP), Pauh Putra Campus, Arau, Perlis, Malaysia
[3]Faculty of Engineering and Technology, Tunku Abdul Rahman University College, Kuala Lumpur, Malaysia
E-Mail: whtan@unimap.edu.my

ABSTRACT

Mobility robot is mostly used by blind and partially sighted people as a mode of transport, leading to more people becoming vulnerable to invisible harm caused by vibration propagated along with the mobility robot structure. Random vibration from different sources propagated along with mobility robot to members of rider body, commonly known as Whole-body Vibration (WBV). Riders commonly experience WBV due to the propagation of vigorous vibration along with the mobility robot footrest. Therefore, vibration analysis is conducted onto the footrest of mobility robot to study its dynamic characteristics corresponding to the excitation frequency induced from the power train of mobility robot. Simulation analysis approach is selected as the method to conduct Finite Element Analysis (FEA). Computer-Aided Drawing (CAD) drafts of the footrest are prepared using CATIA and import the CAD footrest models to ANSYS Workbench to conduct FEA. Two set CAD drafts of footrests are prepared consist of the original and proposed footrest. As a result, it is found that increasing the mass of footrest can reduce the vibration level by more than 93% for X-axis, 70% for Y-axis and 90% for Z-axis. Furthermore, increasing the stiffness of footrest also increased the natural frequencies with the highest increment percentage in the second natural frequency of the proposed footrest, up to 70.12%. In a nutshell, with the increase of mass and designing an appropriate geometry of footrest able to reduce the vibration level significantly.

Keywords: whole-body vibration, finite element analysis, footrest, vibration level, natural frequency.

INTRODUCTION

Vibration is defined as an external force applied continuously on an object. It will cause an object to oscillate back and forth, periodically displaced from its equilibrium position and having the tendency to restore to its equilibrium position. The mechanical vibration experienced by motorcycle riders is known as Whole-Body Vibration (WBV) as the external force sourced from engine mass inertia imbalance and road condition, which transmit the vibration to the members of rider body [1]-[3].

Exposure to whole-body vibration will most likely cause discomfort and unease feeling, which include lower back pain [4] and increase the chances of rider experiencing erectile dysfunction [5], finger and shoulder symptoms [6] under continuous riding circumstances. Vibration transmits from the vibrating sources to the contact points by taking the shortest path at the butt, feet and hand.

Another phenomenon that exerts potential danger is called resonance, where the natural frequency of an object is resonated and induces the object to vibrate at its maximum amplitude [7]. Fortunately, the natural frequency of an object can be altered by changing the material, shape and size of that particular object. The nature of an object, such as the type of material and structure will affect the natural frequency and mode shape. Several studies have been conducted by researchers previously to reduce the vibration level of footrest. Different attempts are used to reduce the vibration level by changing the geometry of footrest in the study of Shashank *et al.* [3] and changing geometry and stiffness by Agostini *et al.* [1]. Other attempts to reduce vibration level is demonstrated by Tan et al. by adding mass to the power tool [8].

Different approaches are used to conduct vibration analysis, including mathematical modelling, experimental measurement and simulation analysis. Researchers commonly develop the mathematical model by neural network using MATLAB, which conducts a learning process based on input data to gain relevant insight to forecast the outcome utilizing the equation of motion [8]-[11]. In experimental measurement, an accelerometer is attached to the object to measure the dynamic properties. Vibrations of the object are induced either by turning on the machine [8] or hit the object by impact hammer [1], [12], [13]. Simulation analysis imports the CAD models to simulation software to conduct Finite Element Analysis (FEA) and determine the dynamic properties of objects [1], [3], [10], [12]. This study aims to determine the dynamic properties of mobility robot original footrest and proposed footrest within the operating frequency range of 17 Hz to 133 Hz. The simulation analysis approach is selected for this study as it is relatively simple and accurate.

Figure-1. Mobility Robot Footrest.

METHODOLOGY

This study consisted of 3 phases which are pre-analysis phase, analysis phase and post-analysis phase. The pre-analysis phase involves collecting the necessary information for vibration analysis, including the geometry of footrest, boundary conditions and system identifications. In the analysis phase, three analyses are conducted: modal analysis, static structural, and harmonic response. Modal analysis is selected to determine the natural mode shapes and frequencies. The mode shape and the amplitude of footrest will be graphically illustrated. Static structural analysis shows the deformation shape and its amplitude when the weight of feet is applied normally to the footrest. Harmonic response determines the steady-state response of the linear structure to loads that vary sinusoidally with time. Results are displayed in the form of vibration level against frequency graph. In the post-analysis phase, the vibration level against frequency graph for both footrests are compared to validate a significant reduction in vibration level for the modified footrest. Finally, the percentage reduction of vibration level is calculated to justify this study.

3D Modelling

Since the left footrest and right footrest are similar, thus the dimension of footrest on one side is taken. The CAD model of footrest is drafted based on Figure 1. The footrest is broken down into three main parts, which are footplate, footrest and foot pedal. The CAD model of original and proposed footrest is drawn as shown in Figure 2. CAD models of original and proposed footrests are drawn on CATIA followed by importing the CAD models to ANSYS Workbench to conduct FEA.

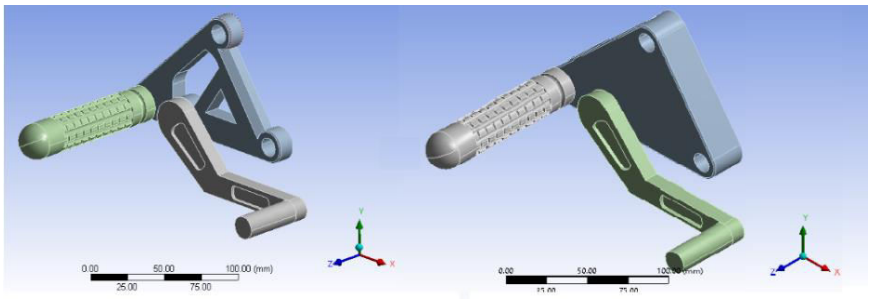

Figure-2. Complete assembly of original (left) and proposed (right) design parts for mobility robot.

Modal Analysis

Boundary conditions and material used for both footrests are the same as well as the settings in ANSYS Workbench remained default to ensure the consistency of study. The fastener holes are fixed as cylindrical supports for both footrests. In modal analysis, the number of modes to be determined is limited to 6 modes only.

Static Structural

The average weight of Malaysian adults is around 62.65kg [14], and the weight exerted by feet onto the surface in contact is approximate 15% of the individual's body weight [15]. Assuming the 15% of body weight is exerted equally onto both feet, 46.10N of weight is exerted normally onto each footrest side. Figure-3 shows the location of vertex point to determine the deformation probe of both footrests. Similar to modal analysis, fastener holes are fixed as cylindrical support. Stiffness can be calculated by substituting relevant data into equation (1):

$$k = \frac{F}{\delta} \quad (1)$$

Where,

k	stiffness
F	force
δ	elongation / deformation amplitude

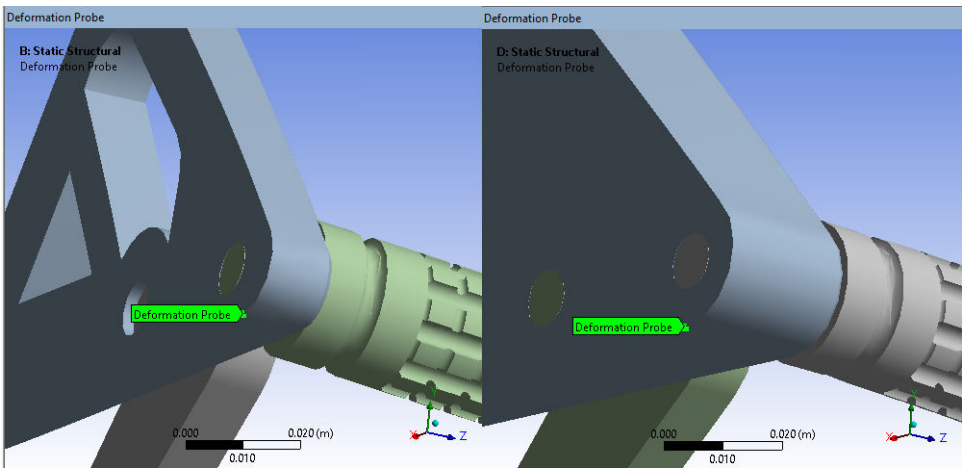

Figure-3. Vertex point of deformation probe.

Harmonic Response

Boundary conditions for harmonic response are similar to previous analyses. Fastener holes are fixed as cylindrical support, and 46.10N weight of feet is assumed to be cyclic load acting normally on the footrest. The frequency range starts from 17 Hz to 133 Hz simulating the operating frequency of a gasoline engine. The response node, which simulates the accelerometer sensor, is placed on the vertex point at the end tip of footrest to record the steady-state response of footrest, as shown in Figure-4.

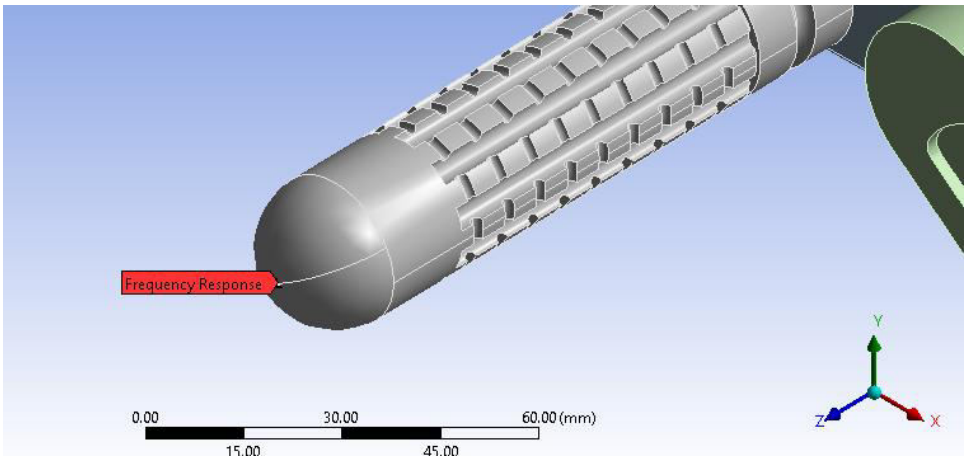

Figure-4. Accelerometer sensor location at vertex point of footrest.

RESULT AND DISCUSSIONS

Modal Analysis

Figure-5 illustrates the total deformation of original footrest for six different modes, and the natural frequencies and maximum deformation amplitude for each mode are tabulated in Table-1. The mode shapes are different from each other when different natural frequencies are resonated. Footrest experienced lateral deflection at a lower frequency and bending at a higher frequency. Deformations mostly occurred at the foot pedal and footrest because these locations are furthest away from the fix supports, which coincide with the modal analysis results of footrest [3] and handlebar [13].

Table-1. Natural frequencies and maximum deformation amplitude of original footrest.

Mode No.	Frequency, Hz	Maximum deformation amplitude, m
1	299.70	0.0668
2	393.58	0.1105
3	527.46	0.0865
4	655.19	0.1496
5	922.19	0.0717
6	1556.90	0.1502

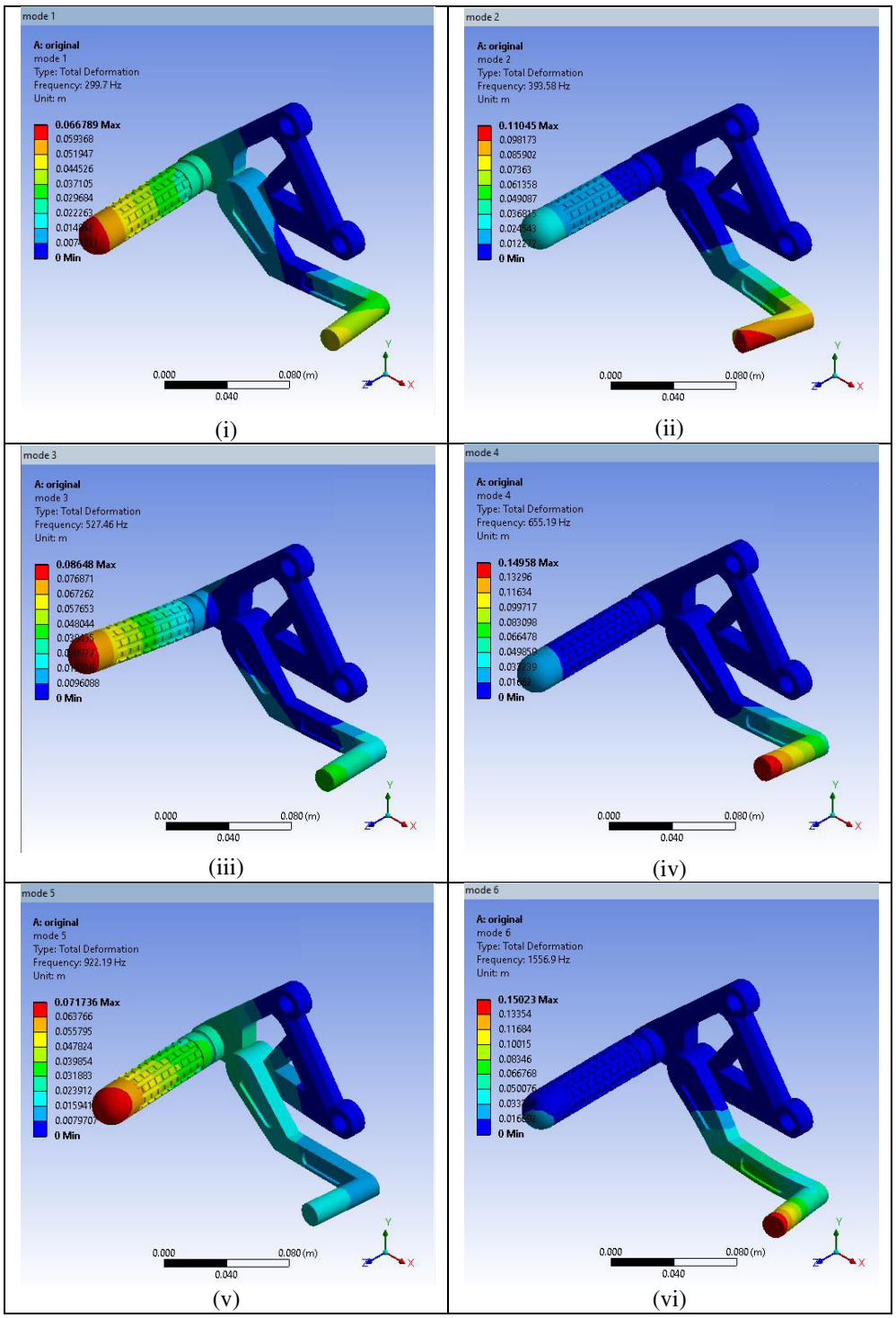

Figure-5. Total deformation of original footrest at (i) 299.70Hz (ii) 393.58Hz (iii) 527.46Hz (iv) 655.19Hz (v) 922.19Hz (vi) 1556.90Hz.

According to the previous study led by Tan *et al.* [8], increasing the object mass enables reducing the amplitude of deformation, which became the inspiration for designing the proposed footrest. Thus, modifying the footplate enables increasing the mass of footrest from 1.2032kg to 2.1671kg, which is almost 1kg heavier than the original footrest. Figure-6 illustrates the total deformation of proposed footrest for six different modes, and Table-2 shows the natural frequencies and maximum deformation amplitude for each mode. The proposed footrest also deformed laterally at a lower frequency similar to the original footrest. The higher frequency proposed footrest experienced bending and twisting at the fifth and sixth frequency mode, respectively. Similarly, deformations frequently occur at the end of foot pedal and footrest.

Table-2. Natural frequencies and maximum deformation amplitude of proposed footrest.

Mode No.	Frequency, Hz	Maximum deformation amplitude, m
1	299.70	0.0668
2	393.58	0.1105
3	527.46	0.0865
4	655.19	0.1496
5	922.19	0.0717
6	1556.90	0.1502

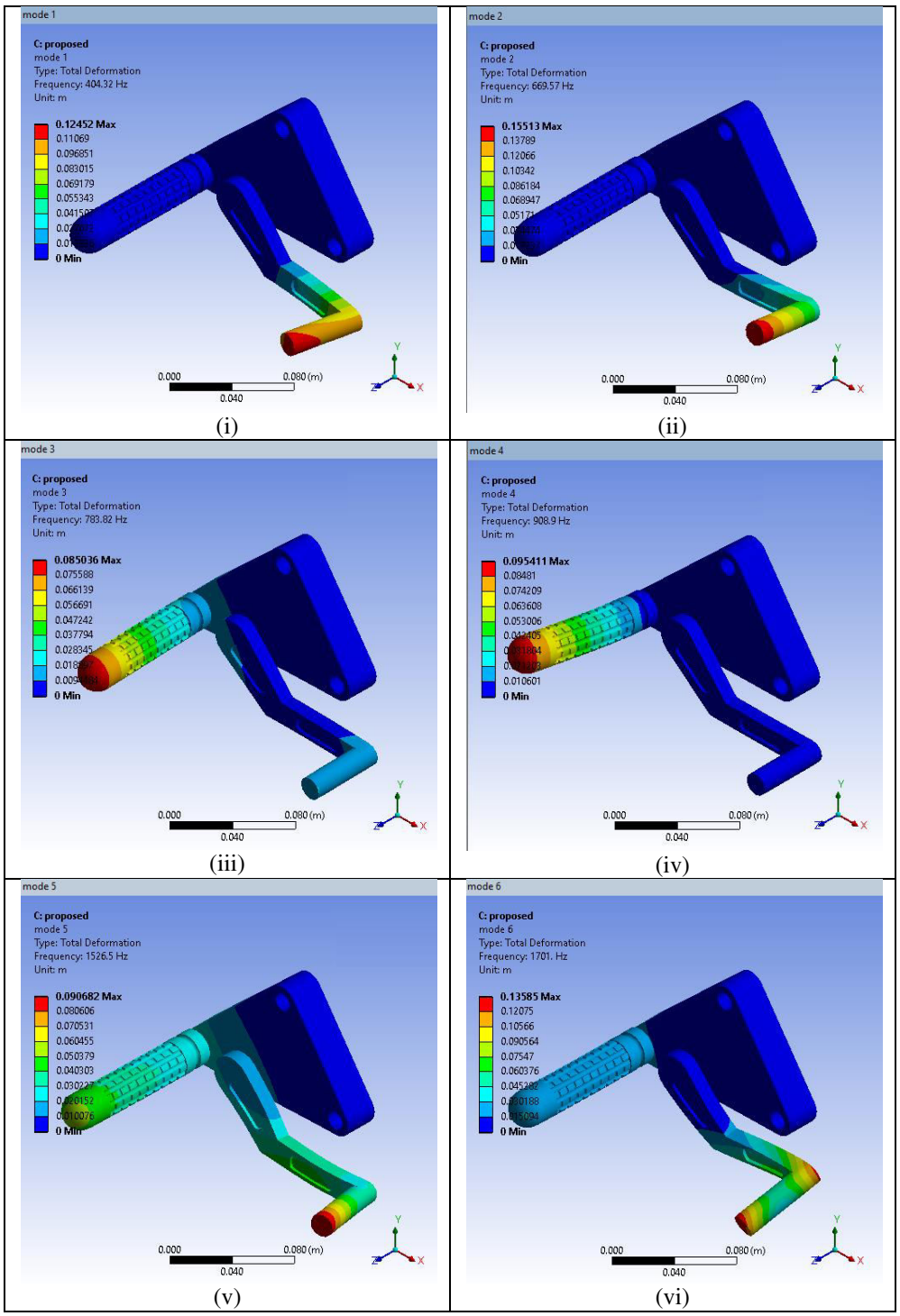

Figure-6. Total deformation of proposed footrest at (i) 404.32Hz (ii) 669.57Hz (iii) 783.82Hz (iv) 908.90Hz (v) 1526.50Hz (vi) 1701.00Hz.

Based on Table-1 and Table-2, the proposed footrest successfully increased the natural frequency in all modes with the highest increment up to 70.12% at the second frequency mode. However, the maximum deformation amplitude of the proposed footrest deformed is greater in the first, second and fifth modes. It should not be a concern since higher natural frequencies are hardly achievable, thus lowering the probability of resonance occur at the lower region of excitation frequency. In a nutshell, modal analysis has identified that both footrests do not experience resonance within the operating frequency range of a small capacity gasoline engine.

Static Structural

The static structural analysis only considered the deformation of footrest when a static load is applied onto the footrest simulating the deformation of footrest when

the rider's feet are stepping on it. Figure-7 shows the mode shape and the maximum deformation amplitude of both footrests. The end of footrest deformed greatest in the negative direction of Y-axis with an amplitude of 2.4463×10^{-5}m and 7.1295×10^{-6}m for the original and proposed footrest. A thicker footplate can reduce the deformation amplitude of footrest up to 70.86% of reduction.

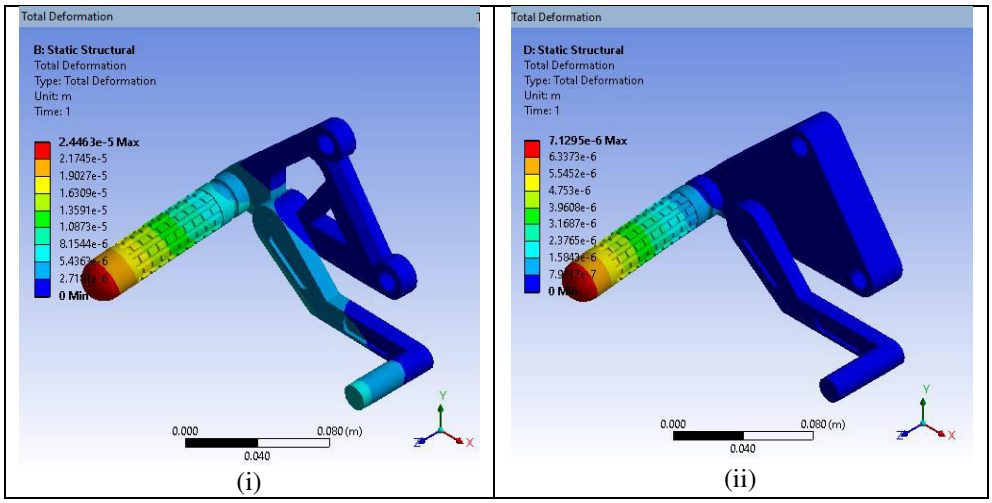

Figure-7. Static deformation of (i) original footrest (ii) proposed footrest.

To determine the stiffness of footrest, a vertex point is located at the bottom of the footplate to identify the deformation probe. The results showed that the amplitudes of the original and proposed footrest deformation probe are 8.08×10^{-6}m and 8.87×10^{-7}m, respectively. Considering the force exerted onto the footrest to be 1N, substituting respective deformation amplitudes into equation (1); hence, the stiffness of footrest is determined, which are 123.76kN/m and 1,127.40kN/m corresponding to the original and proposed footrest. Based on the calculation, the proposed footrest's stiffness is almost 10 times stiffer than the original footrest, which explains why the natural frequency of proposed footrest in each mode is higher than the natural frequency of original footrest.

Harmonic Response

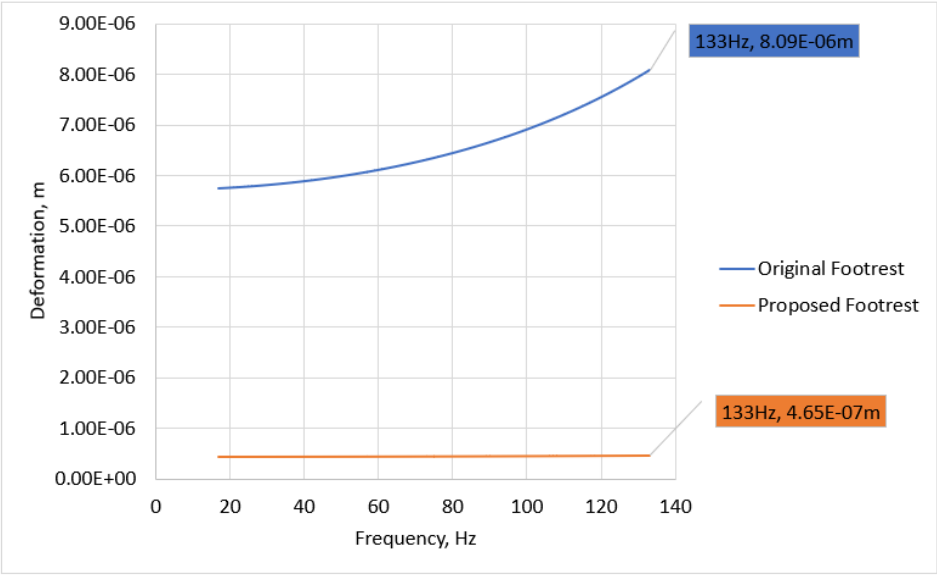

Figure-8. Comparison of harmonic response between both footrests in x-axis in terms of deformation.

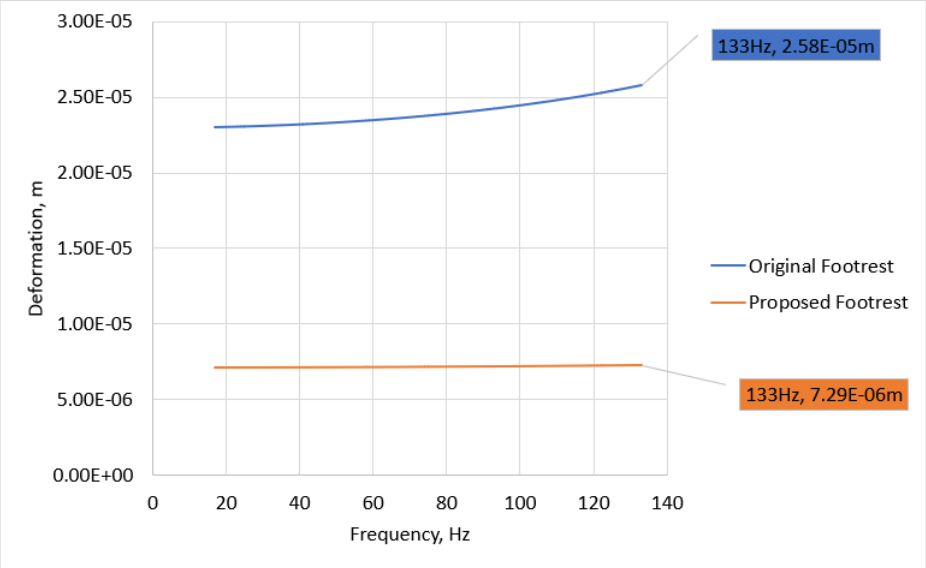

Figure-9. Comparison of harmonic response between both footrests in y-axis in terms of deformation.

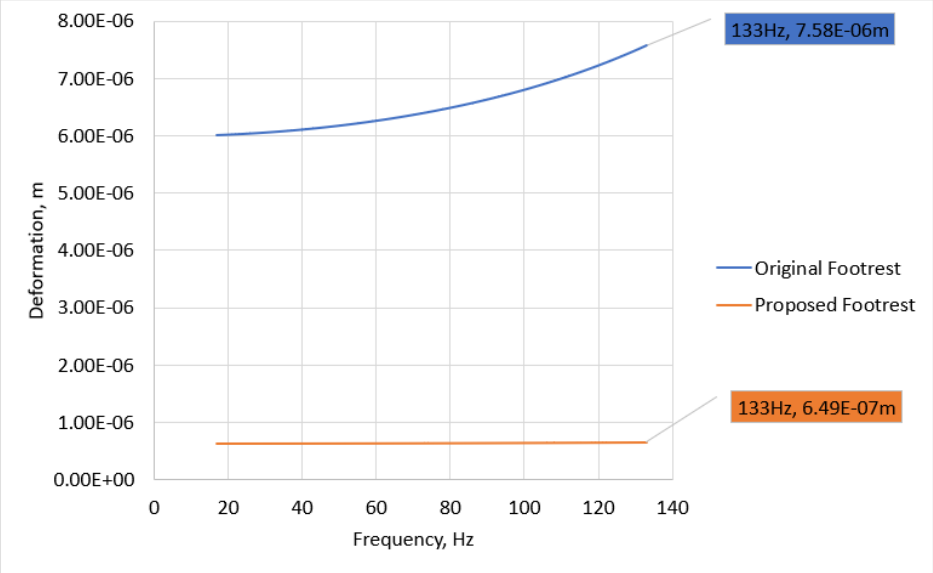

Figure-10. Comparison of harmonic response between both footrests in z-axis in terms of deformation.

Figure-8, Figure-9 and Figure-10 compare the harmonic response between both footrests in terms of deformation in the direction of X, Y and Z axis, respectively for the operating frequency range of small capacity gasoline engine. The increment of vibration levels in all axes are almost uniform, achieving the highest vibration level at 133 Hz. As shown in these figures, the proposed footrest significantly reduced the vibration level in all axes showing an almost flat curve compared to the original design. The increment of deformation amplitude of the proposed footrest is relatively small compared to the original design, which explains why the increment curve of deformation is almost flat. The percentage of reduction in deformation amplitudes in all axes are determined by identifying the root mean square (RMS) deformation amplitudes for both footrests on their axis. In the X-axis, the RMS deformation amplitudes of original and proposed footrest are 6.56×10^{-6}m and 4.44×10^{-7}m, respectively, and the percentage of reduction is 93.23%. At the Y-axis, the RMS deformation amplitudes of original and proposed footrest are 2.40×10^{-5}m and 7.18×10^{-6}m, respectively, and the percentage of reduction is 70.1%. Finally, the RMS deformation amplitudes in Z-axis of the original and proposed footrest are 6.56×10^{-6}m and 6.35×10^{-7}m, respectively, and the percentage of reduction is 90.32%. The proposed footrest has a greater tendency in decreasing vibration levels at X and Z axis. It also shows a lower

tendency in the Y-axis based on the percentage of vibration level reduction in the corresponding axes.

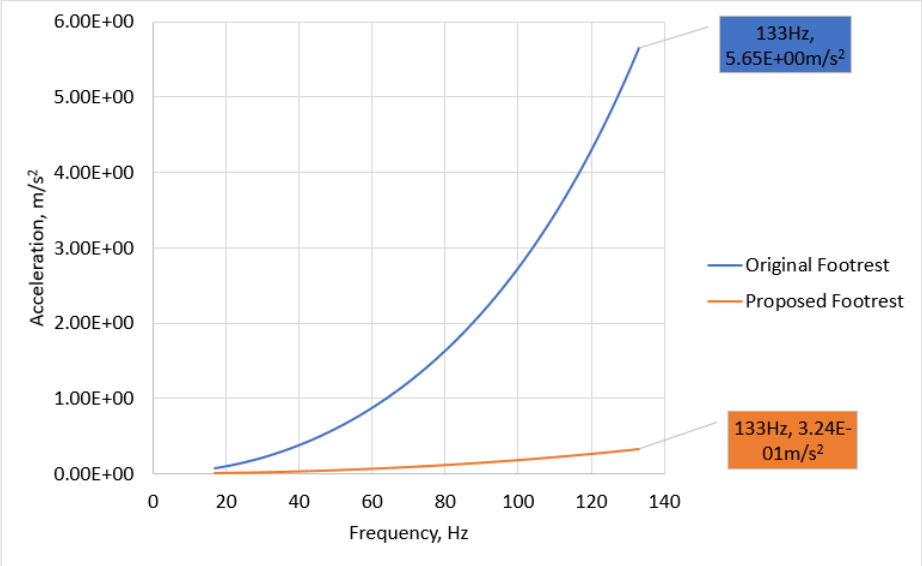

Figure-11. Comparison of harmonic response between both footrests in x-axis in terms of acceleration.

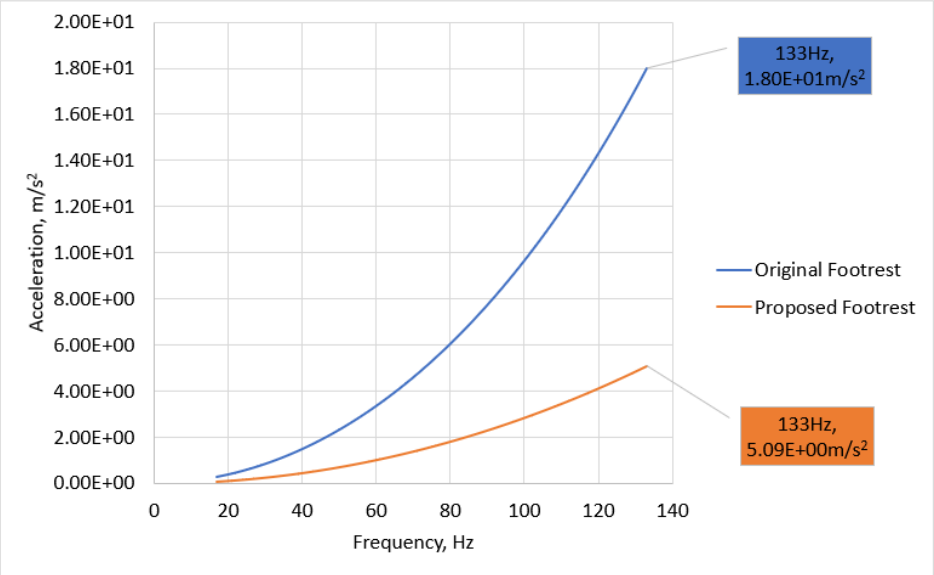

Figure-12. Comparison of harmonic response between both footrests in y-axis in terms of acceleration.

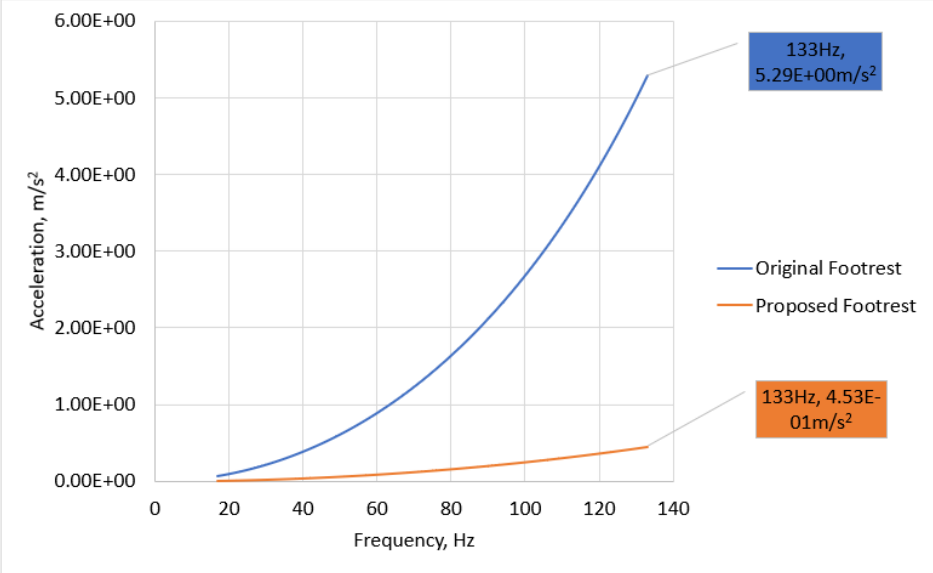

Figure-13. Comparison of harmonic response between both footrests in z-axis in terms of acceleration.

Figure-11, Figure-12 and Figure-13 show the comparison of harmonic response between original and proposed footrest for X, Y and Z axis in terms of acceleration. Similarly, the increment of vibration levels in all axes are almost uniform, achieving the highest vibration level at 133 Hz. Unsurprisingly, the proposed footrest is shown a tremendous reduction in vibration level for all axes. Based on the proposed footrest's harmonic response gradient, the vibration level reduction is more significant for the X and Z axis but not Y-axis. The RMS acceleration amplitudes of the X-axis for both original and proposed footrest are $2.47m/s^2$ and $0.153m/s^2$, respectively, and the percentage of reduction is 93.81%. For Y-axis, the respective RMS acceleration amplitudes of original and proposed footrest are recorded as $8.38m/s^2$ and $2.43m/s^2$, the percentage of reduction is 71%. For Y-axis, the respective RMS acceleration amplitudes of original and proposed footrest are $2.38m/s^2$ and $0.216m/s^2$, the percentage of reduction is 90.92%. The percentage of vibration level reduction justified that the proposed footrest tends to reduce the vibration level in the X and Z-axis compared with the Y-axis.

CONCLUSIONS

In this study, increasing the mass footrest and changing its geometry reduced the vibration level and increased the stiffness of proposed footrest, which led to an increased natural frequency of proposed footrest for each mode. Regardless the physical characteristics of both footrests, both footrests exert similar dynamic characteristics according to the modal analysis, where both footrests deformed laterally in a direction showing uniform mode shapes at lower mode natural frequency. As the mode frequency getting higher, footrests started to deform vigorously in different directions, such as bending or twisting. The absence of vibration level peak in harmonic response indicated no resonance within the operating frequency range for both footrests. This result is validated where modal analysis showed the first mode frequency of original and proposed footrest are 299.70Hz and 404.32Hz, which significantly higher than the maximum operating frequency of a small capacity gasoline engine. The harmonic response of both footrests also illustrated the dominant deformation is occurred at Y-axis. Comparing the vibration levels between both footrests for different axes concluded that the proposed footrest reduced the vibration level significantly compared to the original footrest. ISO 2631-1 [16] suggested that the range of frequency considered unharmful to humans is between 0.5Hz and 80Hz.

ACKNOWLEDGMENT

The research has been carried out under the Malaysian Technical University Network (MTUN) Research Grant by Ministry of Higher Education of Malaysia (MOHE) under a grant number of (9028-00005) & (9002-00089) with the research collaboration with thanks to the Center of Excellence Automotive & Motorsport and Faculty of Mechanical Engineering Technology, Universiti Malaysia Perlis (Malaysia) for their productive discussions and input to the research。

REFERENCES

[1] S. Agostoni, F. Cheli, E. Leo and M. Pezzola. 2012. Methodology to design a vibration absorption footplate for motorcycle application: From phenomena investigation to prototype performance evaluation. Mech. Syst. Signal Process. 30: 296-305.

[2] D. J. Kalsule, R. R. Askhedkar and P. R. Sajanpawar. 1999. Engine induced vibration control for a motorcycle chassis frame by right combination of

finite element method and experimental techniques. SAE Tech. Pap. (724).

[3] S. Shashank, K. S. Teja, S. V. Adithya and K. L. Hari. 2013. Experimental analysis of vibration in a motorcycle footrest. 1(3): 35-42.

[4] M. J. Griffin. 1990. Handbook of Human Vibration 1990. London, San Diego: Elsevier Ltd.

[5] A. Ochiai *et al*. 2006. Do motorcyclists have erectile dysfunction? A preliminary study. Int. J. Impot. Res. 18(4): 396-399.

[6] H. C. Chen, W. C. Chen, Y. P. Liu, C. Y. Chen and Y. T. Pan. 2009. Whole-body vibration exposure experienced by motorcycle riders - An evaluation according to ISO 2631-1 and ISO 2631-5 standards. Int. J. Ind. Ergon. 39(5): 708-718.

[7] R. K. Mobley. 1999. Vibration Fundamental, 1st ed. Elsevier Science & Technology.

[8] W. H. Tan, E. A. Lim and K. S. Ong. 20196. Analysis of Vibration Level for Power Tool Using Neural Network. Int. J. AUTOMOTIVE Mech. Eng. 16(3): 7121-7132.

[9] W. H. Tan, J. X. Cheah, C. K. Lam, E. A. Lim, H. G. Chuah, and C. Y. Khor. 2017. Vibration analysis on compact car shock absorber. J. Phys. Conf. Ser. 908(1).

[10] M. A. B. Marzuki, M. H. A. Halim and A. R. N. Mohamed. 2015. Determination of natural frequencies through modal and harmonic analysis of space frame race car chassis based on ANSYS. Am. J. Eng. Appl. Sci. 8(4): 538-548.

[11] K. Taylor. 2017. Neural Networks Using Matlab, Function Approximation and Regression. Create Space Independent Publishing Platform.

[12] P. A. Borse and P. S. Desale. 2017. Design and Vibrational Analysis of Motorcycle Handlebar by FEA Method and correlating it with Test Results. 4(7): 291-296.

[13] S. Chomphan. 2019. Vibration signal analysis of a motorcycle. Int. J. GEOMATE. 16(56): 27-32.

[14] M. Y. Azmi *et al*. 2009. Body mass index (BMI) of adults: Findings of the Malaysian Adult Nutrition Survey (MANS). Malays. J. Nutr. 15(2): 97-119.

[15] H. Hirschfeld, M. Thorsteinsdottir and E. Olsson. 1999. Coordinated ground forces exerted by buttocks and feet are adequately programmed for weight transfer during sit-to-stand. J. Neurophysiol. 82(6): 3021-3029.

[16] Y. Marjanen and N. Mansfield. 2010. Validation and improvement of the ISO 2631-1 (1997) standard method for evaluating discomfort from whole-body vibration in a multi-axis environment. vol. Ph.D. p. 283.